tvst

Special Issue

Corneal Optical Coherence Tomography Speckle in Crosslinked and Untreated Rabbit Eyes in Response to Elevated Intraocular Pressure

Monika E. Danielewska[1], Agnieszka Antończyk[2], Danilo Andrade De Jesus[3], Maja M. Rogala[4], Anna Błońska[5], Marek Ćwirko[5], Zdzisław Kiełbowicz[2], and D. Robert Iskander[1]

[1] Wrocław University of Science and Technology, Department of Biomedical Engineering, Wrocław, Poland
[2] Wrocław University of Environmental and Life Sciences, Department of Surgery, Faculty of Veterinary Medicine, Wrocław, Poland
[3] Erasmus University Medical Center, Department of Radiology and Nuclear Medicine, Biomedical Imaging Group Rotterdam, Rotterdam, The Netherlands
[4] Wrocław University of Science and Technology, Department of Mechanics, Materials and Biomedical Engineering, Wrocław, Poland
[5] Ophthalmology Clinical Centre SPEKTRUM, Wrocław, Poland

Correspondence: Monika E. Danielewska, Wrocław University of Science and Technology, Department of Biomedical Engineering, Wybrzeże Wyspiańskiego 27, 50-370 Wrocław, Poland. e-mail: monika.danielewska@pwr.edu.pl

Received: July 23, 2020
Accepted: November 9, 2020
Published: April 29, 2021

Keywords: corneal crosslinking; inflation experiment; intraocular pressure; corneal OCT speckle; tissue characterization

Citation: Danielewska ME, Antończyk A, Andrade De Jesus D, Rogala MM, Błońska A, Ćwirko M, Kiełbowicz Z, Iskander DR. Corneal optical coherence tomography speckle in crosslinked and untreated rabbit eyes in response to elevated intraocular pressure. Transl Vis Sci Technol. 2021;10(5):2, https://doi.org/10.1167/tvst.10.5.2

Purpose: To ascertain the influence of intraocular pressure (IOP) on corneal optical coherence tomography (OCT) speckle in untreated and ultraviolet A–riboflavin induced corneal collagen crosslinked rabbit eyes.

Methods: Left corneas of eight rabbits were de-epithelialized and crosslinked by applying riboflavin and 30-minute ultraviolet A light exposure. After enucleation (6 months after treatment), each eyeball (treated and untreated) was mounted in a measurement setup, in which IOP was increased from 15 to 45 mm Hg in steps of 5 mm Hg. At each IOP value, single B-scans of the central cornea were acquired three times with the spectral-domain OCT Copernicus-HR. Then, three regions of interest, including the anterior, posterior, and entire corneal stroma, were automatically extracted. Five different probability distributions were used as a model for the corneal speckle and the one with the best goodness of fit was chosen for further analysis.

Results: The generalized gamma distribution achieved the best goodness of fit and its scale (a) and shape (v) parameters statistically significantly changed with increasing IOP in the three regions of analysis (two-way repeated measures analysis of variance, all $P < 0.05$). The statistically significant difference between untreated and crosslinked eyes was observed for the shape parameters of the posterior and entire corneal stroma.

Conclusions: Corneal OCT speckle is influenced by IOP and shows to be significantly different in untreated and crosslinked eyes. Corneal OCT speckle analysis has the potential to be indirectly used for assessing changes in corneal stroma in ex vivo and in vivo studies.

Translational Relevance: Investigation of corneal OCT speckle statistics can offer additional diagnostic biomarkers related to changes in the corneal stroma after ocular surgeries.

Introduction

The cornea is continuously subjected to the load of intraocular pressure (IOP). Its structure can undergo irreversible changes related to the natural aging process,[1] pathologic conditions such as keratoconus,[2] eye diseases associated with the elevation of IOP as glaucoma,[3] or being a result of refractive surgery.[4] In the case of keratoconic eyes, topographic alterations occur owing to biomechanical changes in corneal structure.[5] As a consequence of those changes, corneal

elasticity and rigidity are affected.[2] Subsequently, the cornea may become weaker and more susceptible to variations in IOP. In turn, in eyes with an elevated IOP, structural alterations of the cornea occur and lead to the increase of corneal rigidity.[6,7] Visualizing the microstructural properties of the cornea in vivo is a challenging task. Hence, there is an unmet need to find reliable parameters that will be useful clinically in assessing those properties in ocular disorders.

Monitoring these changes in corneal properties requires long-term studies. One of the methods to investigate short duration changes in the corneal properties is an inflation test. There are several animal and human inflation experiments, including those performed in vivo and ex vivo, showing the molecular rearrangement and increase of corneal stiffness as a response to the IOP elevation.[6,8] The advantage of ex vivo tests is the ability to fully control the true IOP values[9] and to assess additional corneal biomechanical properties, which, in turn, are inaccessible in noninvasive in vivo studies.

Another way to change the properties of the cornea is to use collagen crosslinking that induces intrafibrillar and interfibrillar covalent bonds and hence, increases corneal stiffness.[10–12] Corneal crosslinking with riboflavin used as a photosensitizer is a surgical treatment for keratoconus and other ectatic corneal conditions.[13,14] Its effect was found to be the most pronounced in the anterior one-half of the stroma.[11]

Several methods have been developed to measure biomechanical properties of the cornea[2,9] and to visualize corneal microstructure.[11,15,16] However, most of them can be applied only ex vivo and, as such, have multiple limitations related to tissue dissection or setting the experimental conditions that do not accurately reflect the natural physiological conditions, such as temperature, ocular tissue hydration, and ocular pulsation. Nevertheless, nondestructive and in vivo quantifying microstructure of the cornea is of clinical significance. Recently, an in vivo technique of statistically modeling optical coherence tomography (OCT) speckle showed the potential to assess age-related changes in the corneal microstructure and those induced by corneal swelling.[17]

Furthermore, indirect parameterization of corneal microstructure acquired in vivo, based on the light intensity distribution in the corneal Scheimpflug images, similar to OCT, was shown to differentiate eyes with mild keratoconus from control ones.[18] Following this observation, the aim of our study was to ascertain whether corneal OCT speckle is influenced by an increase in IOP and whether speckle statistics can differentiate rabbit eyes treated with riboflavin–ultraviolet-A–induced collagen crosslinking from the fellow untreated eyes.

Methods

Animals

The study protocol for the experimental use of the animals was approved by the Animal Care and Ethics Committee of the Wroclaw University of Environmental and Life Sciences (No. 82/2017) and adhered to the guidelines of the ARVO Statement for the Use of Animals in Ophthalmic and Vision Research.

Eight New Zealand white rabbits weighing from 3.1 to 3.7 kg and aged 6 months at the study onset were enrolled. The rabbits were acclimatized for 2 weeks after shipment in single stainless steel cages under standard environmental conditions. The rabbits were fed a commercial diet (Labofeed KH Standard) and had ad libitum access to water. All rabbits were clinically healthy. Before the experiment, each rabbit underwent an ophthalmologic examination. No corneal opacity, eye discharge, ulceration, or other ophthalmic abnormalities were noted.

Corneal Crosslinking Treatment

The corneal crosslinking procedure was conducted under general anesthesia and local analgesia of the left treated eye, primarily for minimizing postoperative discomfort. Rabbits were premedicated with acepromazine (0.5 mg/kg; Calmivet, Vétoquinol, Luré, France) and midazolam (0.5 mg/kg, Midanium, Polfa Warszawa S.A., Poland). Propofol was used to induce general anesthesia (Propofol-Lipuro 1%, B. Braun Melsungen AG, Germany) at an initial dose of 0.5 mg/kg. Following larynx local analgesia (Lignocainum Hydrochloricum WZF 2%, Polfa), rabbits were intubated and general anesthesia was maintained with oxygen-volatilized isoflurane (1.5–2.0 vol.%, IsoVet, Piramal Healthcare, UK). Directly before treatment, the topical ophthalmic local anesthetic (proxymetacaine [Alcaine] ophthalmic drops 0.5%, Alcon, Bornem, Belgium) was applied to the conjunctival sac to provide an adequate level of analgesia.

The left eyes were crosslinked, while the right untreated eyes were used as controls. The central 8 mm of the left corneas were de-epithelialized completely by gently scraping them with the EBK epikeratome Epi Clear (Orca Surgical, One World Trade Center, New York, NY). A 0.1% riboflavin solution containing 10% dextran (Ribocross TE, IROS Srl, Napoli, Italy) was applied to the debrided central corneas

5 minutes before the irradiation. Then, the corneas were treated by 30 minutes of ultraviolet A light exposure with an irradiance of 3 mW/cm^2 using LightLink CXL Corneal Cross-Linking System (LIGHTMED USA, San Clemente, CA) with a wavelengths of 370 nm (total energy dose of 5.4 J/cm^2), at a focusing distance of 5 cm from the cornea surface and an illumination diameter of 8 mm. During the irradiation, riboflavin was reapplied at 5-minute intervals. The crosslinking treatment protocol was compatible with the one previously described in rabbit eyes.[12]

Measurement of the Central Corneal Thickness (CCT)

Before epithelial debridement and after ultraviolet A light exposure, the CCT of the treated eye was measured using an ultrasonic pachymeter (Pocket II Echograph Pachymeter, Quantel Medical, France).

Inflation Test

Six months after treatment, the animals were humanely euthanized. At first, all rabbits were anesthetized with an intramuscular injection of medetomidine (0.3 mg/kg, Cepetor, CP-Pharma Handelsges, Germany) and ketamine (20 mg/kg, Bioketan, Vetoquinol Biowet, Poland). Subsequently, the anesthesia was deepened by intravenous injection of pentobarbital (Morbital, Biowet Puławy, Poland) at an initial dose of 50 mg/kg, to effect. The rationale behind choosing 6 months as a time point for ex vivo study was to avoid CCT as a potential confounding factor in the corneal OCT speckle analysis because the biological healing process after crosslinking is relatively lengthy and includes, e.g., changes in corneal hydration and CCT values, as well as stromal repopulation.[19,20]

Immediately after enucleation of both eyes (treated and untreated), each eyeball was transported in a storage medium of phosphate-buffered saline (PBS) solution at 4 °C and then mounted in a custom-made holder of the measurement setup, less than 1 hour post mortem. The holder limited eyeball movements, but did not come in direct contact with the eye tissues, because it was separated from them with a delicate layer of cotton wool soaked in PBS. The stable and fixed position of the eye in the holder was additionally secured with polyamide sewing thread connecting the optic nerve to the holder frame. To control corneal swelling for ex vivo study inclusion, each treated and untreated eyeball was examined using a slit-lamp biomicroscope and its CCT was measured using IOL Master 700 biometer (Carl Zeiss Meditec AG, Jena, Germany). During the measurements, the eye was regularly moistened using PBS to maintain proper hydration of the cornea.

To control IOP, a 19G needle was inserted into the anterior chamber through the corneoscleral limbus area. The needle was connected to a pressure transmitter (WIKA, Klingenberg am Main, Germany) with relative pressure range of 0 to 187.5 mm Hg (0.05% accuracy class) and a custom-made syringe pump. The IOP value was increased stepwise from 15 to 45 mm Hg in increments of 5 mm Hg and monitored continuously by the pressure transmitter and a computer with a specially developed software for controlling the pumping process. More technical details regarding this software as well as the scheme illustrating the measurement setup are given in our earlier study.[21]

The ex vivo experiments of each pair of rabbit eyes were completed within 2.5 hours of enucleation. The order of measuring the crosslinked and control rabbit eyeballs was randomized to minimize any bias resulted from changes in corneal hydration.

OCT Image Acquisition and Processing

The spectral-domain OCT Copernicus HR (OPTOPOL, Zawiercie, Poland) was used to acquire the images. The center wavelength, axial, and lateral resolutions of the device were 850 nm, 3 µm, and 15 µm, respectively. The images were sampled through 1024 A-scans with 848 pixels per A-scan at the speed of 25000 A-scans per second. For each eye and at each IOP value, a single B-scan image of the cornea, covering its central area, was acquired three times. The B-scan width was set to 4 mm to maximize its transversal resolution. Each image was acquired at the same axial position within the bands of instrument's depth of focus.

The OCT B-scans were inverse-log transformed and normalized to a range of 0 to 1. Epithelium, endothelium, and the Bowman's layer were automatically detected with the method described by Jesus et al.[17] Then three regions of interest (ROIs) were automatically extracted from the corneal stroma. The first region, denoted as aROI, was limited to the anterior corneal stroma, and selected between the Bowmans' layer and middle of the stroma thickness. The second region, denoted as pROI, was limited to the posterior corneal stroma, and was selected between the middle of the stroma thickness and the endothelium, and the third region, denoted as ROI, included the entire central corneal stroma. The horizontal dimension of each ROI was limited to the central 2 mm of the available field of view to decrease any potential effect of

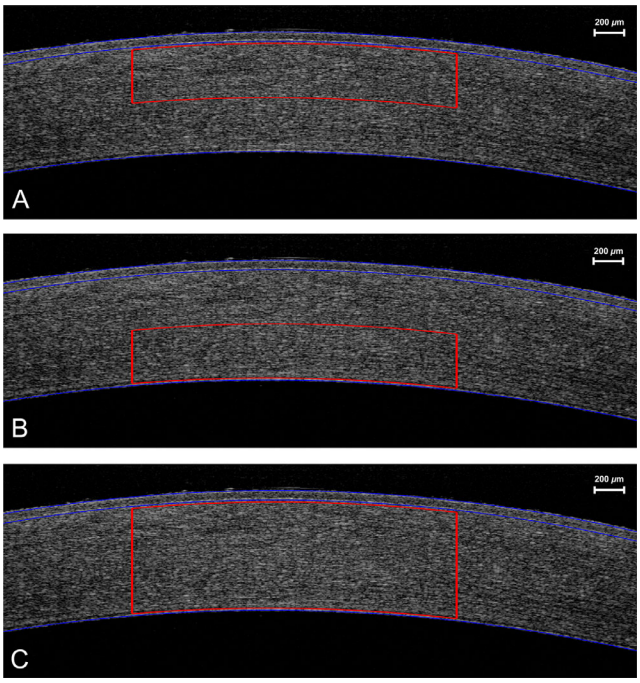

Figure 1. An example of a corneal OCT B-scan of the untreated eye with three ROIs: the anterior corneal stroma, aROI (A), the posterior corneal stroma, pROI (B), and the entire central corneal stroma, ROI (C), delineated in red color.

corneal curvature on the imaged speckle. The vertical dimension of each ROI depended on the thickness of the stroma. The rationale behind considering three ROIs was the results of earlier studies that presented the most pronounced effect of crosslinking in the anterior one-half of the stroma in rabbits[11] and changes in the regional collagen lamellae architecture with the IOP increase in isolated rabbit corneas.[16] Figure 1 shows an example of a B-scan with the aROI, pROI, and ROI delineated in red.

Preliminary Analysis

Several probabilistic models have been applied for speckle modeling in OCT images. In the recent study, the generalized gamma distribution, among several other models considered, has been shown to optimally fit the human corneal OCT speckle.[17] In this study, the statistics of rabbit corneal speckle were investigated by fitting probability distribution functions to the pixel intensities of the transformed and normalized earlier B-scans in each of the three selected ROIs and each considered IOP level. Specifically Rayleigh, Gamma, Weibull, Nakagami, and Generalized Gamma distributions were considered as they were found to effectively model both ultrasound examination and OCT speckle.[17,22–27] In a preliminary step, the goodness-of-fit (GoF) of each model was estimated by calculating the mean squared error between the fitted probability density function and the kernel density estimator. Figure 2 shows that GOF for the three considered ROIs and the seven levels of IOP for untreated and treated eyes, whereas in Figure 3, illustrative histograms of corneal speckle for pROI of a crosslinked eyes are shown against the five estimated probability density functions for the lowest and highest considered levels of IOP (i.e., 15 mm Hg and 45 mm Hg). Because the generalized gamma distribution showed the best overall average GOF among the five considered distributions and it was also statistically significantly different from the other considered models (Wilcoxon test, all pairs $P < 0.001$; see Fig. 4), it was used as the statistical model of the corneal OCT speckle in further analyses. The probability density function of generalized gamma distribution is given by:

$$f(x; a, v, p) = \frac{|p|}{\Gamma(v)\, a^{pv}} x^{pv-1} \exp\left\{\left(-\frac{x}{a}\right)^{p}\right\},$$

where a is the scale parameter (in units of normalized amplitude), v and $p \neq 0$ (both in arbitrary units) are the shape parameters, $x \geq 0$ is the pixel intensity, and Γ is the conventional gamma function.[28] The scale parameter has been proposed to indicate the average backscattered power, whereas the ratio of the shape parameters (v/p) to indicate scatter density.[27]

Statistical Analysis

Statistical analyses consisted of standard descriptive statistics and the two-way repeated measures analysis of variance (ANOVA) to determine the main effects of IOP, treatment, and interaction between these variables (denoted as IOP × treatment) on the values of generalized gamma distribution parameters. The significance level was set to an α of 0.05. To validate the assumption of sphericity of repeated measures ANOVA, the Mauchly sphericity test was used, whereas a Greenhouse–Geisser adjustment was applied to correct for violations of sphericity. If a significant main effect or interaction was found, Bonferroni corrected post hoc tests were performed. Additionally, to compare the CCT values of the treated eyes before and after treatment, as well as the CCT values between untreated and crosslinked enucleated eyes, the paired two-tailed t-test was applied. Calculations were performed using SPSS 22.0 (SPSS, Inc., Chicago, IL).

Results

Illustrative examples of corneal OCT B-scans of untreated and crosslinked corneas for the lowest and

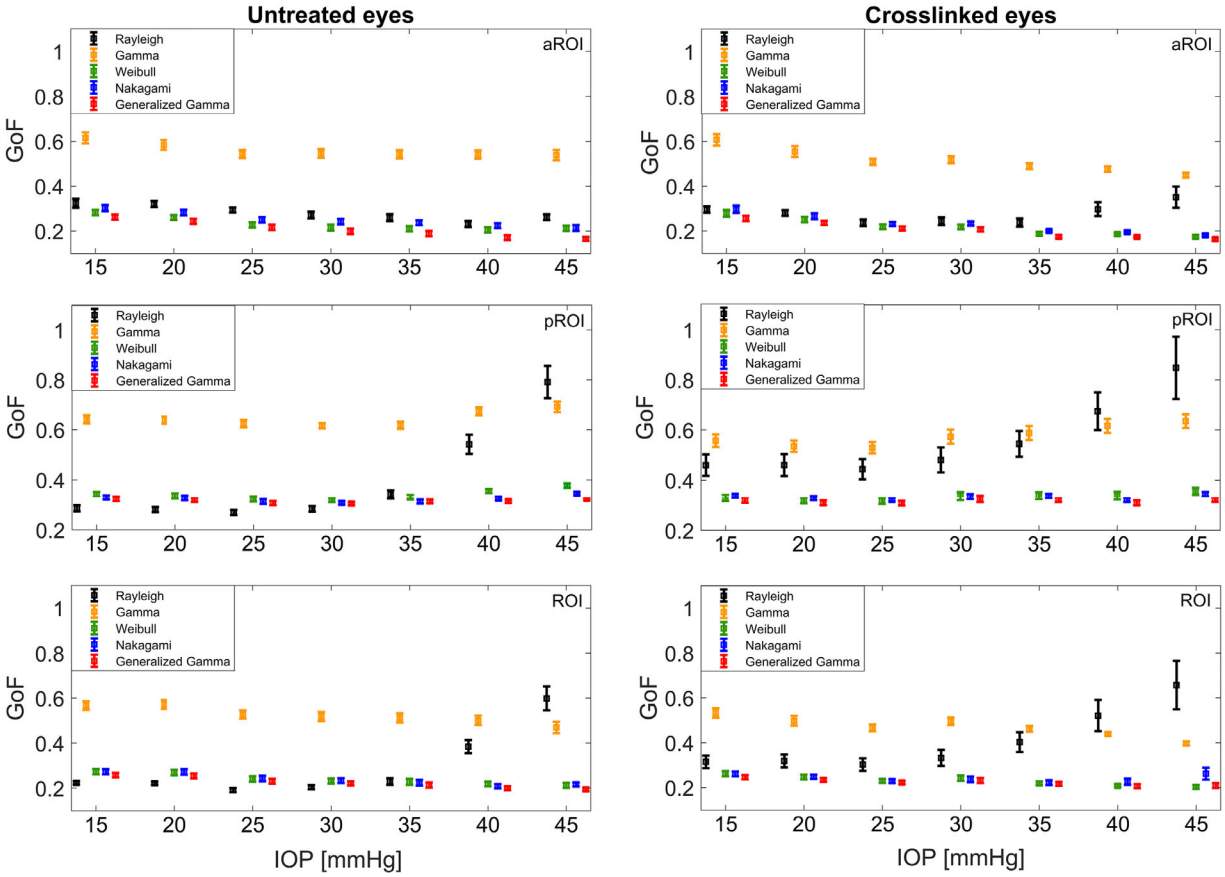

Figure 2. Group means and corresponding standard errors of the GOF of five probabilistic models (Rayleigh, Gamma, Weibull, Nakagami, and Generalized Gamma distributions) fitted to the pixel intensities of the rabbit corneal OCT images acquired for the untreated (*left*) and crosslinked (*right*) eyes for the anterior, posterior, and entire central corneal stroma (i.e., aROI, pROI, and ROI, respectively) at seven considered levels of IOP.

highest considered levels of IOP (i.e., 15 mm Hg and 45 mm Hg) with an enlarged view of their stroma are presented in Figure 5.

The results of the two-way repeated measures ANOVA for IOP, treatment, and interactions between IOP and treatment performed for the three regions of

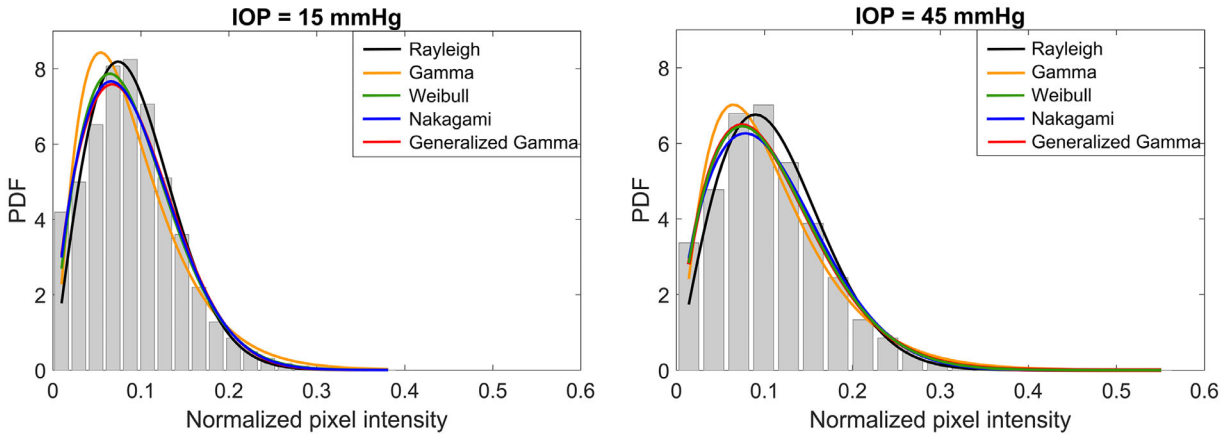

Figure 3. Illustrative histograms of corneal OCT speckle for the posterior corneal stroma of a crosslinked eye and the fitted five probability density functions (PDF) for two levels of IOP: 15 mm Hg (*left*) and 45 mm Hg (*right*).

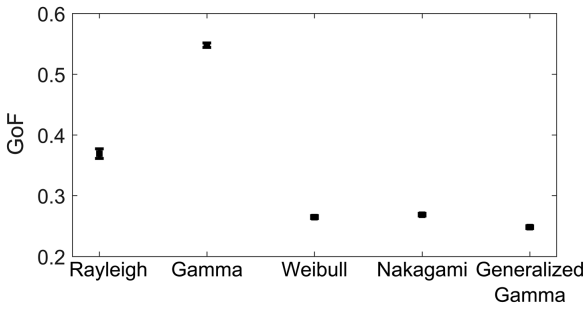

Figure 4. The overall averages and corresponding standard errors of the GOF of the five statistical models (Rayleigh, Gamma, Weibull, Nakagami, and Generalized Gamma distributions) calculated for measurements of both eyes, all IOP values and for all three ROIs.

the OCT scans (aROI, pROI, and ROI) were gathered in the Table. Mauchly's test of sphericity indicated that this assumption was not met for IOP and interaction IOP × treatment for all parameters in all regions; therefore, a Greenhouse–Geisser correction was used for the *F*-ratio computations.

The scale (a) and both shape parameters (v, p) of the fitted distribution in the untreated and crosslinked eyes were found to change in a statistically significantly manner with increasing IOP in the three regions of analysis, except for the p parameter in the posterior corneal stroma (see IOP row in the Table). The highest value of partial eta squared (η^2) of the parameter a shows the largest main effect of the IOP elevation in the anterior corneal stroma. Also, the additionally considered ratio of the shape parameters, v/p, was found to change significantly with increasing IOP in the anterior and posterior corneal stroma ($P < 0.001$ and $P = 0.010$, respectively).

Statistically significant differences between untreated and crosslinked eyes were observed for the p parameter for all considered regions of cornea (all $P < 0.05$). Additionally, in the posterior and entire regions of corneal stroma the v parameter and the ratio v/p differentiated both groups of eyes (see Treatment row in the Table).

Table. Summary of Two-Way Repeated Measures ANOVA for IOP and Treatment Conditions

		Parameters											
		a			*v*			*p*			*v/p*		
ROI in OCT Image	Variables	*F*	*P* Value	η^2	*F*	*P* Value	η^2	*F*	*P* Value	η^2	*F*	*P* Value	η^2
aROI	IOP	*F*(2.668, 61.373) = 95.311	<0.001*	0.806	*F*(2.836, 65.231) = 29.732	<0.001*	0.564	*F*(2.106, 48.427) = 6.417	0.003*	0.218	*F*(2.640, 60.724) = 16.761	<0.001*	0.422
	Treatment	*F*(1,23) = 0.842	0.368	0.035	*F*(1,23) = 0.038	0.847	0.002	*F*(1,23) = 6.233	0.020*	0.213	*F*(1,23) = 1.632	0.214	0.066
	IOP × Treatment	*F*(3.645, 83.831) = 2.684	0.042*	0.104	*F*(2.089, 48.048) = 2.594	0.083	0.101	*F*(2.895, 66.587) = 2.429	0.075	0.096	*F*(2.423, 55.732) = 2.147	0.117	0.085
pROI	IOP	*F*(1.969, 45.284) = 37.377	<0.001*	0.619	*F*(2.828, 65.033) = 14.849	<0.001*	0.392	*F*(3.099, 71.280) = 1.988	0.122	0.080	*F*(2.610, 60.038) = 4.353	0.010*	0.159
	Treatment	*F*(1,23) = 4.958	0.036*	0.177	*F*(1,23) = 10.790	0.003*	0.319	*F*(1,23) = 11.684	0.002*	0.337	*F*(1,23) = 15.315	0.001*	0.400
	IOP × Treatment	*F*(1.362, 31.330) = 4.573	0.030*	0.166	*F*(1.580, 36.350) = 1.445	0.247	0.059	*F*(1.584, 36.438) = 3.257	0.061	0.124	*F*(1.537, 35.359) = 2.746	0.090	0.107
ROI	IOP	*F*(1.840, 42.328) = 14.673	<0.001*	0.389	*F*(2.740, 63.018) = 18.256	<0.001*	0.443	*F*(1.625, 37.374) = 9.999	0.001*	0.303	*F*(2.218, 51.015) = 1.880	0.159	0.076
	Treatment	*F*(1,23) = 3.064	0.093	0.118	*F*(1,23) = 12.724	0.002*	0.356	*F*(1,23) = 13.829	0.001*	0.375	*F*(1,23) = 16.454	<0.001*	0.417
	IOP × Treatment	*F*(1.465, 33.686) = 0.699	0.461	0.030	*F*(2.409, 55.401) = 3.346	0.034*	0.127	*F*(1.896, 43.606) = 0.562	0.565	0.024	*F*(2.508, 57.695) = 1.922	0.146	0.077

[a]ROI, anterior corneal stroma; pROI, posterior corneal stroma; ROI, entire central corneal stroma; *a*, *v*, *p*: parameters of the generalized gamma distribution.

F stands for *F*-ratio and it is reported as *F* (degrees of freedom, error of degrees of freedom), η^2 denotes partial *eta* squared and is a measure of effect size, whereas the asterisk denotes statistically significant results. The numbers of the degrees of freedom of the F-distribution not expressed as integers indicate that the sphericity assumption was not valid and that the Greenhouse-Geisser correction was used.

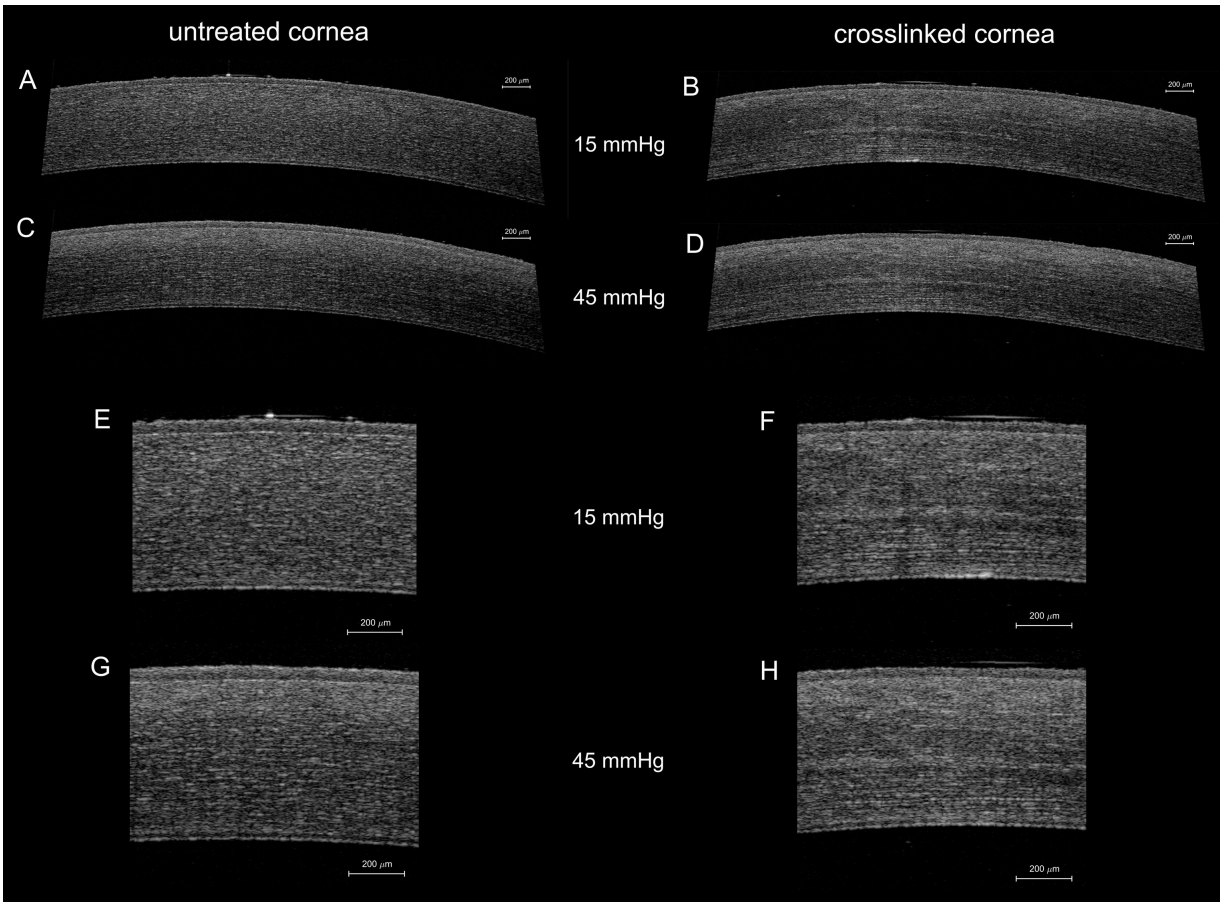

Figure 5. Illustrative examples of corneal OCT B-scans of untreated (A, C) and crosslinked (B, D) corneas for the IOP of 15 mm Hg and 45 mm Hg with enlarged views of their stroma (E, G and F, H, respectively).

The results of the two-way repeated measures ANOVA revealed statistically significant main effects ($P < 0.05$) of interaction between the IOP and treatment on values of the a parameter in the anterior and posterior corneal stroma, whereas in the entire region of central corneal stroma, the corresponding main effect was observed for the v parameter (see IOP × Treatment row in the Table). Figures 6, 7, and 8 present the four considered parameters as functions of IOP in the untreated and crosslinked rabbit eyes for the three considered regions of the central corneal stroma, respectively.

In the in vivo experiment, mean values of CCT decreased statistically significantly (t-test; $P = 0.046$) from the mean value of 382 ± 26 μm before epithelial debridement to 363 ± 26 μm after the treatment with a 0.1% riboflavin–dextran solution and ultraviolet A light irradiation. These measurements correspond to the thickness of cornea with and without the epithelium, respectively. The difference between those CCT values cannot be unambiguously related to the corneal abrasion alone, because it depends on the type of the used riboflavin and its properties. This result is in agreement with the study of Zaheer et al.,[29] in which isotonic riboflavin with dextran caused a significant decrease in corneal thickness. Before the ex vivo experiment, there was no statistically significant difference in CCT values between the untreated and the crosslinked enucleated eyes (mean, 511 ± 31 μm vs. 509 ± 38 μm, respectively; t-test $P = 0.776$).

Discussion

The performed inflation experiment revealed that simple models such as the Rayleigh distribution or the gamma distribution do not adequately represent the corneal OCT speckle for the entire considered range of IOP values, whereas models that involve a larger number of parameters sufficiently well model that speckle for both low and high values of IOP achieving similar levels of GOF. Nevertheless, the generalized

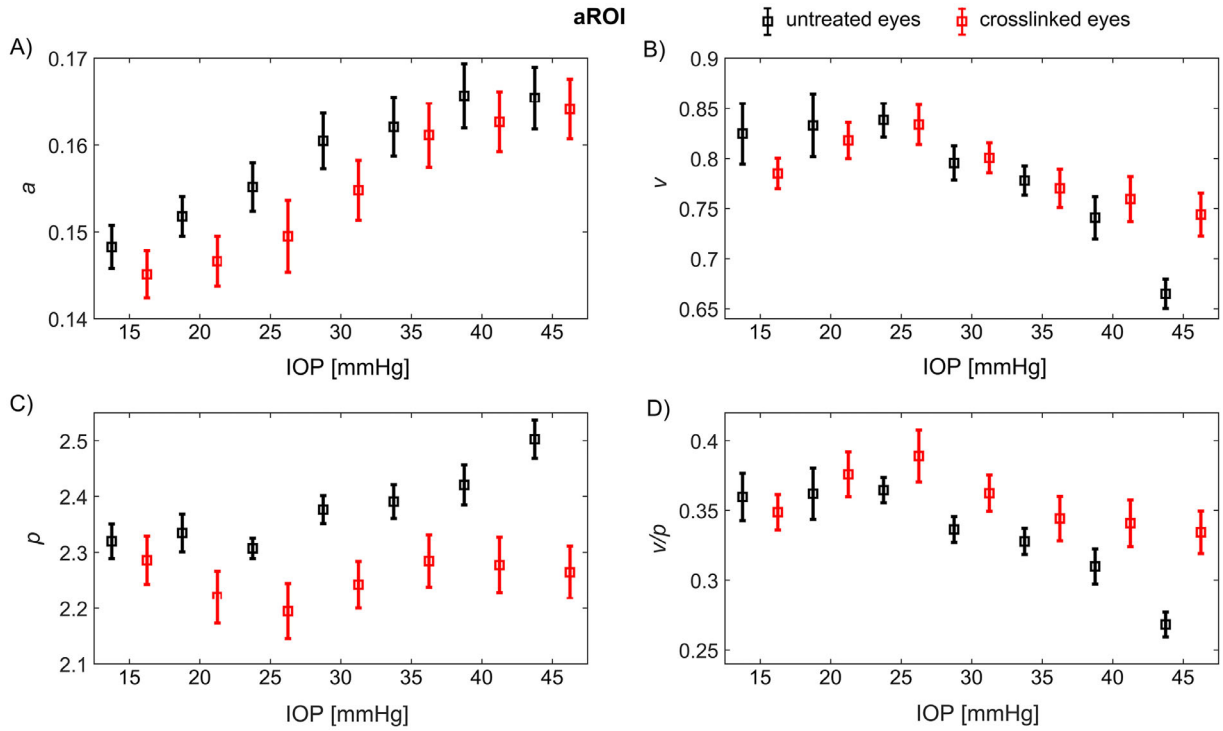

Figure 6. Changes in the group mean and corresponding standard errors of the scale (A) and the shape (B, C) parameters, and the ratio of both shape parameters (D) of corneal OCT speckle of the anterior corneal stroma (aROI) in untreated (*black*) and crosslinked (*red*) rabbit eyes for different IOP values.

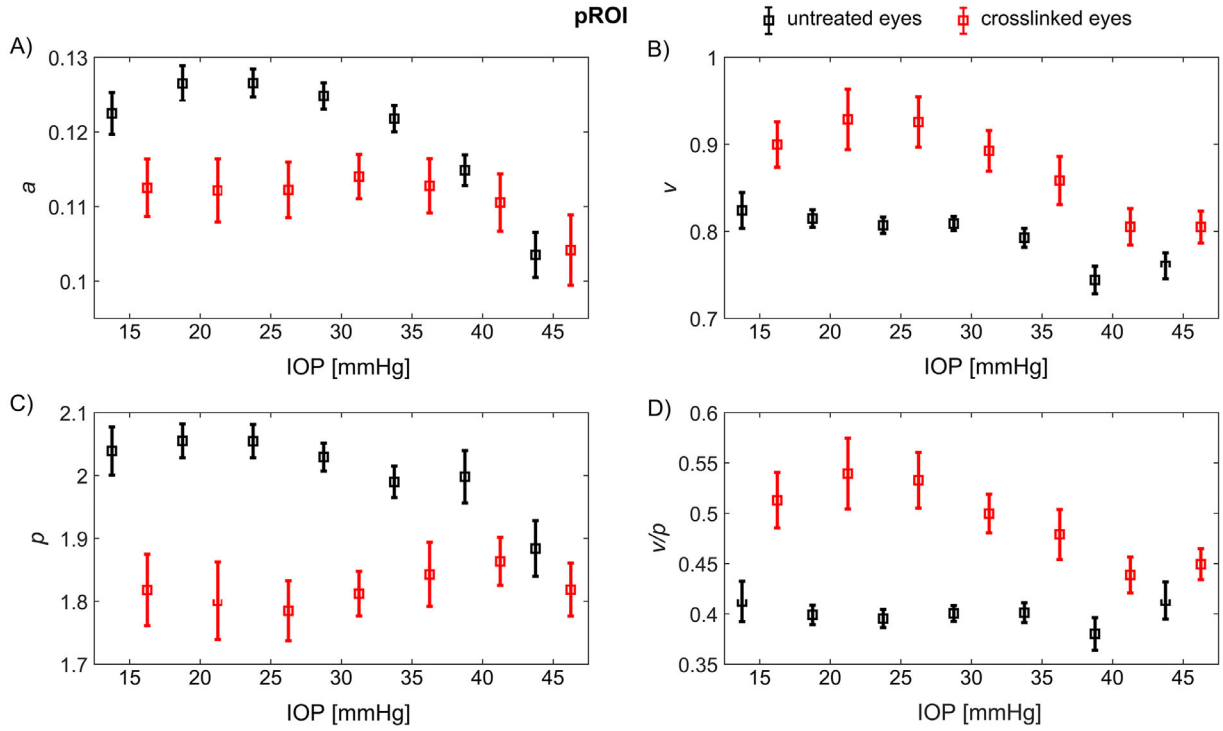

Figure 7. Changes in the group mean and corresponding standard errors of the scale (A) and the shape (B, C) parameters, and the ratio of both shape parameters (D) of corneal OCT speckle of the posterior corneal stroma (pROI) in untreated (*black*) and crosslinked (*red*) rabbit eyes for different IOP values.

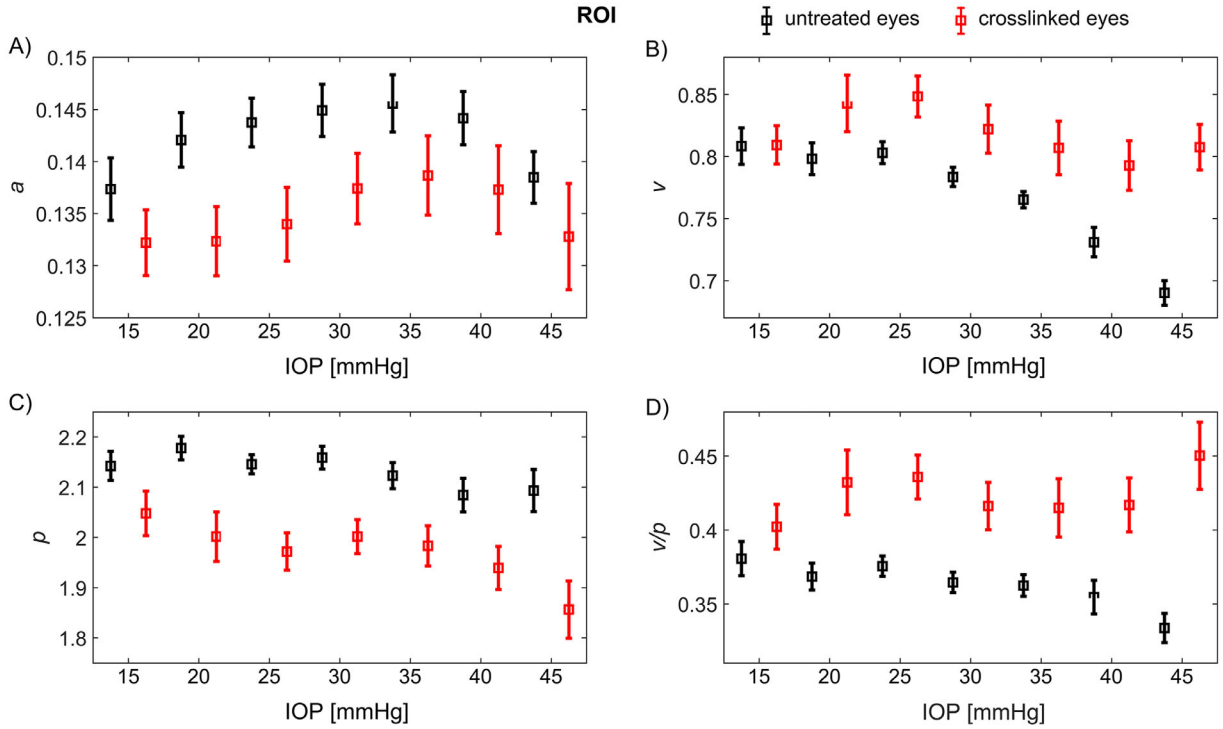

Figure 8. Changes in the group mean and corresponding standard errors of the scale (A) and the shape (B, C) parameters, and the ratio of both shape parameters (D) of corneal OCT speckle of the entire central corneal stroma in untreated (*black*) and crosslinked (*red*) rabbit eyes for different IOP values.

gamma distribution, having three parameters, achieved the best overall GOF.

The obtained results showed the three parameters of the generalized gamma distribution (i.e., *a*, *v*, and *p*) statistically significantly change with IOP. These changes were observed in both the untreated and the treated rabbit eyes, mainly in the anterior and the entire regions of the central corneal stroma. The largest main effect of the IOP on these parameters and the ratio *v*/*p* in the anterior stroma can be explained by changes in its microstructure.[16] In the study by Wu et al.,[16] it was observed using nonlinear optical microscopy that regional collagen lamellae architecture varies with tension in isolated rabbit corneas. Specifically, gaps between the lamellar structures were shown to decrease in size with an increasing IOP. This response of collagen morphology was depth dependent (more visible in the anterior central stroma). Also, nonlinear optical imaging allowed observation of the reorganization of the collagen lamellae during the mechanical inflation test on intact fresh human corneas.[30] The current study provides an indirect evidence supporting those developments, obtained with OCT, a clinically accessible technique of coarser resolution than that of nonlinear optical microscopy, but having the potential to be indirectly used for assessing corneal stroma in ex vivo and in vivo studies.

Furthermore, in the entire region of the corneal stroma, the scatter density (the *v* parameter) differentiates untreated from crosslinked eyes, taking into account the IOP, whereas in the anterior and posterior regions, the average backscatter power (the *a* parameter) has this property. Corneal stiffening owing to crosslinking is characterized by collagen structural changes leading to an increased resistance to pressure load. However, it is challenging to distinguish these changes from those linked to increasing values of IOP without any reliable physical parameters related to the tissue stiffness.[31] Therefore, given these findings, it can be hypothesized that all parameters of corneal OCT speckle analyzed here are indirect indicators of the corneal microstructural response to incremental changes in IOP.

The results of this study demonstrated that the corneal OCT speckle statistics distinguished untreated and crosslinked eyes based on the shape parameter (*p*) in all considered regions of the corneal stroma. However, the obtained higher main effect of treatment on the *p* parameter, and in addition on the *a* and *v* parameters, in the posterior corneal stroma than in the

anterior one can indicate a difference in optical scattering in both corneal regions resulted from the transition zone between the crosslinked anterior corneal stroma and the untreated posterior corneal stroma. In keratoconus patients after crosslinking, this zone, defined as a stromal demarcation line,[32] was visualized at 1 month postoperatively using anterior segment OCT[33] and even earlier than 3 weeks after treatment using ultrahigh-resolution OCT.[34] In this study, at 6 months after crosslinking and immediately after enucleation, a characteristic, however inhomogeneous, transition zone in the OCT images of treated corneas has been identified in six of the eight rabbits.

Earlier animal studies have shown the anterior localization of the crosslinking effect[11,35,36] including, such as changes in the swelling behavior of the corneal anterior stroma.[36] This phenomenon has also been observed in humans as a transient post-treatment effect and the corneas have regained their normal hydration level in the long term.[37] In the current study, the normal hydration state of rabbit corneas after enucleation is assumed based on statistically insignificant differences between the CCT values of the untreated and treated eyeballs. Furthermore, taking into account time-dependent postmortem changes in animal eyes and some ex vivo experimental conditions (i.e., eyeball bathing in PBS) it is likely that these factors might also have had a potential impact on a discrepancy in corneal speckle statistics. However, it is presumed that the transition zone, altering the scattering properties within this region in treated eyes, could contribute to the major effect on differences in the values of generalized gamma parameters between the crosslinked and control eyes in the posterior corneal stroma.

Corneal microstructural and biomechanical changes, as a result of crosslinking treatment, are associated with a relative long-term biological healing process (including the epithelial restoration and stromal recovery) within months after the procedure.[12,31,38,39] For example, Bueno et al.[38] reported that crosslinking modifies the arrangement of the collagen fibers at different corneal depth locations in rabbit corneas after 4 weeks of in vivo treatment. Furthermore, Wollensak et al.[12] showed an increase in corneal stiffness maintained up to 8 months after crosslinking of rabbit corneas. In the current study, the crosslinking treatment was carried out in in vivo conditions and then the OCT imaging of the rabbit corneas was performed 6 months after the procedure, when the confounding factor of CCT was supposed to be minimized. The results of this study confirmed the validity of this approach because the mean CCT values of untreated and crosslinked enucleated eyes did not differ significantly. Hence, it can be anticipated that the healing process after photopolymerization contributes to the observed here alterations in the corneal OCT speckle statistics. In addition, the analysis of corneal OCT speckle statistics has the potential to offer additional diagnostic biomarkers, related to changes in corneal stroma and biomechanics undergoing in corneal healing processes after surgical interventions.

Furthermore, aging influences the architectural changes of the corneal stroma.[1] In human corneas, an increase in the cross-sectional areas of collagen fibrils[40] and fibrillar molecules[41] was reported with age as a potential result of an increase in nonenzymatic crosslinking. Also, the age-related changes were observed in the generalized gamma parameters of the corneal speckle distribution, where a and p decreased with age, whereas the v increased with age.[17] According to the study of Doughty et al.,[42] who examined rabbits aged between 3 and 36 months, the CCT increases steadily with age. Hence, any potential increase in CCT of crosslinked corneas at 6 months could have also contributed to changes in the corneal speckle statistics.

One of the limitations of this study is the small sample size. Nevertheless, the differences in the corneal OCT speckle statistics between treated and untreated eyes, as well as between different levels of IOP, were not only statistically significant, but also had a large main effect. Furthermore, there was no opportunity to measure the CCT of the untreated eye during the crosslinking procedure because of the supine head position of the rabbit. Monitoring CCT values throughout the ex vivo experiment could have been beneficial to evaluate the potential changes in CCT with increasing IOP and their potential impact on the corneal OCT speckle. However, technical difficulties prohibited this option. Therefore, more studies are needed to assess these mutual relationships. Considering the width of the ROI, it is important to note that it may bias the results, particularly because of the corneal curvature. Here it was chosen at 2 mm central to the corneal apex to minimize that effect. The interpretations obtained here and their comparisons with human studies should be made with caution owing to the many anatomical and biomechanical differences between human and rabbit eyes, as well as the different experimental conditions (i.e., extracted corneas vs. entire eyeball, time after treatment).

In conclusion, corneal OCT speckle statistics distinguish untreated rabbit corneas from those after crosslinking and show that both corneas react to an increase in IOP. Hence, analysis of the OCT speckle has the potential to provide, in an indirect and noninvasive way, information on the corneal stroma and be a valuable biomarker in clinical practice to monitor

postoperative changes in corneal stroma caused by ocular surgeries.

Acknowledgments

The work of M. E. Danielewska and D. R. Iskander has been funded by the National Science Centre, Poland, OPUS Grant 2018/29/B/ST7/02451.

Disclosure: **M.E. Danielewska,** None; **A. Antończyk,** None; **D. Andrade De Jesus,** None; **M.M. Rogala,** None; **A. Błońska,** None; **M. Ćwirko,** None; **Z. Kiełbowicz,** None; **D.R. Iskander,** None

References

1. Geraghty B, Whitford C, Boote C, Akhtar R, Elsheikh A. Age-related variation in the biomechanical and structural properties of the corneoscleral tunic. In: Derby B, Akhtar R, eds. *Mechanical Properties of Aging Soft Tissues. Engineering Materials and Processes*. Cham, Switzerland: Springer. 2015:207–235.
2. Shah S, Laiquzzaman M, Bhojwani R, Mantry S, Cunliffe I. Assessment of the biomechanical properties of the cornea with the ocular response analyzer in normal and keratoconic eyes. *Invest Ophthalmol Vis Sci*. 2007;48(7):3026–3031.
3. Brown KE, Congdon NG. Corneal structure and biomechanics: impact on the diagnosis and management of glaucoma. *Curr Opin Ophthalmol*. 2006;17(4):338–343.
4. Pepose JS, Feigenbaum SK, Qazi MA, Sanderson JP, Roberts CJ. Changes in corneal biomechanics and intraocular pressure following LASIK using static, dynamic, and noncontact tonometry. *Am J Ophthalmol*. 2007;143(1):39–47.e1.
5. Piñero DP, Alio JL, Barraquer RI, Michael R, Jiménez R. Corneal biomechanics, refraction, and corneal aberrometry in keratoconus: an integrated study. *Invest Ophthalmol Vis Sci*. 2010;51(4):1948–1955.
6. Clayson K, Pan X, Pavlatos E, et al. Corneoscleral stiffening increases IOP spike magnitudes during rapid microvolumetric change in the eye. *Exp Eye Res*. 2017;165:29–34.
7. Dastiridou AI, Ginis HS, de Brouwere D, Tsilimbaris MK, Pallikaris IG. Ocular rigidity, ocular pulse amplitude, and pulsatile ocular blood flow: the effect of intraocular pressure. *Invest Ophthalmol Vis Sci*. 2009;50:5718–5722.
8. Bell JS, Hayes S, Whitford C, et al. The hierarchical response of human corneal collagen to load. *Acta Biomater*. 2018;65:216–225.
9. Bao F, Deng M, Wang Q, et al. Evaluation of the relationship of corneal biomechanical metrics with physical intraocular pressure and central corneal thickness in ex vivo rabbit eye globes. *Exp Eye Res*. 2015;137:11–17.
10. Wollensak G, Spoerl E, Seiler T. Stress-strain measurements of human and porcine corneas after riboflavin-ultraviolet-A-induced cross-linking. *J Cataract Refract Surg*. 2003;29(9):1780–1785.
11. Wollensak G, Wilsch M, Spoerl E, Seiler T. Collagen fiber diameter in the rabbit cornea after collagen crosslinking by riboflavin/UVA. *Cornea*. 2004;23(5):503–507.
12. Wollensak G, Iomdina E. Long-term biomechanical properties of rabbit cornea after photodynamic collagen crosslinking. *Acta Ophthalmol*. 2009;87(1):48–51.
13. Wollensak G, Spoerl E, Seiler T. Riboflavin/ultraviolet-a–induced collagen crosslinking for the treatment of keratoconus. *Am J Ophthalmol*. 2003;135(5):620–627.
14. Iseli HP, Thiel MA, Hafezi F, Kampmeier J, Seiler T. Ultraviolet A/riboflavin corneal cross-linking for infectious keratitis associated with corneal melts. *Cornea*. 2008;27(5):590–594.
15. McQuaid R, Li J, Cummings A, Mrochen M, Vohnsen B. Second-harmonic reflection imaging of normal and accelerated corneal crosslinking using porcine corneas and the role of intraocular pressure. *Cornea*. 2014;33(2):125–130.
16. Wu Q, Yeh AT. Rabbit cornea microstructure response to changes in intraocular pressure visualized by using nonlinear optical microscopy. *Cornea*. 2008;27(2):202–208.
17. Jesus DA, Iskander DR. Assessment of corneal properties based on statistical modeling of OCT speckle. *Biomed Opt Express*. 2017;8(1):162–176.
18. Consejo A, Gławdecka K, Karnowski K, et al. Corneal properties of keratoconus based on Scheimpflug light intensity distribution. *Invest Ophthalmol Vis Sci*. 2019;60(8):3197–3203.
19. Greenstein SA, Shah VP, Fry KL, Hersh PS. Corneal thickness changes after corneal collagen crosslinking for keratoconus and corneal ectasia: one-year results. *J Cataract Refract Surg*. 2011;37(4):691–700.
20. Mazzotta C, Balestrazzi A, Traversi C, et al. Treatment of progressive keratoconus by riboflavin-UVA-induced cross-linking of corneal collagen. *Cornea*. 2007;26(4):390–397.

21. Rogala MM, Lewandowski D, Detyna J, Antończyk A, Danielewska ME. Corneal pulsation and biomechanics during induced ocular pulse. An ex-vivo pilot study. *PLoS One*. 2020;15(2):e0228920.
22. Mcheik A, Batatia H, Spiteri P, Tauber C, George J, Lagarde JM. *Skin OCT Images Characterization based on speckle distribution*. Hackensack, NJ: World Scientific Pub Co Pte Lt; 2009:86–95.
23. Lindenmaier AA, Conroy L, Farhat G, DaCosta RS, Flueraru C, Vitkin IA. Texture analysis of optical coherence tomography speckle for characterizing biological tissues in vivo. *Opt Lett*. 2013;38(8):1280–1282.
24. Zaitsev VY, Matveev LA, Matveyev AL, Gelikonov G V, Gelikonov VM. A model for simulating speckle-pattern evolution based on close to reality procedures used in spectral-domain OCT. *Laser Phys Lett*. 2014;11(10):105601.
25. Raju BI, Srinivasan MA. Statistics of envelope of high-frequency ultrasonic backscatter from human skin in vivo. *IEEE Trans Ultrason Ferroelectr Freq Control*. 2002;49(7):871–882.
26. Caixinha M, Jesus DA, Velte E, Santos MJ, Santos JB. Using ultrasound backscattering signals and Nakagami statistical distribution to assess regional cataract hardness. *IEEE Trans Biomed Eng*. 2014;61(12):2921–2929.
27. Tunis AS, Czarnota GJ, Giles A, Sherar MD, Hunt JW, Kolios MC. Monitoring structural changes in cells with high-frequency ultrasound signal statistics. *Ultrasound Med Biol*. 2005;31(8):1041–1049.
28. Stacy EW, Mihram GA. Parameter estimation for a generalized gamma distribution. *Technometrics*. 1965;7(3):349–358.
29. Zaheer N, Khan WA, Khan S, Khan MAM. Comparison of changes in central corneal thickness during corneal collagen cross-linking, using isotonic riboflavin solutions with and without dextran, in the treatment of progressive keratoconus. *Cornea*. 2018;37(3):340–346.
30. Benoit A, Latour G, Marie-Claire SK, Allain JM. Simultaneous microstructural and mechanical characterization of human corneas at increasing pressure. *J Mech Behav Biomed Mater*. 2016;60:93–105.
31. Touboul D, Gennisson JL, Nguyen TM, et al. Supersonic shear wave elastography for the in vivo evaluation of transepithelial corneal collagen cross- linking. *Invest Ophthalmol Vis Sci*. 2014;55(3):1976–1984.
32. Mazzotta C, Wollensak G, Raiskup F, Pandolfi AM, Spoerl E. The meaning of the demarcation line after riboflavin-UVA corneal collagen crosslinking. *Expert Rev Ophthalmol*. 2019;14(2):115–131.
33. Doors M, Tahzib NG, Eggink FA, Berendschot TTJM, Webers CAB, Nuijts RMMA. Use of anterior segment optical coherence tomography to study corneal changes after collagen cross-linking. *Am J Ophthalmol*. 2009;148(6):844–851.e2.
34. Pantalon A, Pfister M, Aranha dos Santos V, et al. Ultrahigh-resolution anterior segment optical coherence tomography for analysis of corneal microarchitecture during wound healing. *Acta Ophthalmol*. 2019;97(5):e761–e771.
35. Kohlhaas M, Spoerl E, Schilde T, Unger G, Wittig C, Pillunat LE. Biomechanical evidence of the distribution of cross-links in corneas treated with riboflavin and ultraviolet a light. *J Cataract Refract Surg*. 2006;32(2):279–283.
36. Wollensak G, Aurich H, Pham DT, Wirbelauer C. Hydration behavior of porcine cornea crosslinked with riboflavin and ultraviolet A. *J Cataract Refract Surg*. 2007;33(3):516–521.
37. Holopainen JM, Krootila K. Transient corneal thinning in eyes undergoing corneal cross-linking. *Am J Ophthalmol*. 2011;152(4):533–536.
38. Bueno JM, Ávila FJ, MC Martínez-Garciá. Quantitative analysis of the corneal collagen distribution after in vivo cross-linking with second harmonic microscopy. *Biomed Res Int*. 2019;2019:3860498.
39. Bradford SM, Mikula ER, Juhasz T, Brown DJ, Jester J V. Collagen fiber crimping following in vivo UVA-induced corneal crosslinking. *Exp Eye Res*. 2018;177:173–180.
40. Daxer A,, Misof K,, Grabner B,, Ettl A,, Fratzl P. Collagen fibrils in the human corneal stroma: structure and aging. *Invest Ophthalmol Vis Sci*. 1998;39(3):644–648.
41. Malik NS, Moss SJ, Ahmed N, Furth AJ, Wall RS, Meek KM. Ageing of the human corneal stroma: structural and biochemical changes. *BBA - Mol Basis Dis*. 1992;1138(3):222–228.
42. Doughty MJ. The cornea and corneal endothelium in the aged rabbit. *Optom Vis Sci*. 1994;71(12):809–818.